Solution Phase Conformational Studies of the Cyclic Peptide RA-VII: Lithium Chloride Perturbation of the Conformational Equilibria

Dale L. Boger,* Michael A. Patane, and Jiacheng Zhou

Contribution from the Department of Chemistry, The Scripps Research Institute, 10666 North Torrey Pines Road, La Jolla, California 92037

Received March 31, 1995[⊗]

Abstract: The conformations and conformational equilibria of RA-VII and related natural products in THF-d_8 were found to be similar to that observed in conventional solvents ($CDCl_3$, 15% CD_3OD−$CDCl_3$). The addition of 1 equiv of LiCl resulted in the adoption of a single dominant solution conformation (94%) that corresponds to the major conformation detected in conventional solvents ($CDCl_3$, CD_3OD, DMSO-d_6, THF-d_8), and the further addition of LiCl (2−12 equiv) had no additional effect on the structure or conformational equilibria of the agent. The LiCl complexed solution conformation in THF-d_8 closely resembles the X-ray structure conformation. This conformation contains a characteristic and diagnostic cis C^{30}−N^{29} *N*-methyl amide central to a type VI β-turn and the rigid cycloisodityrosine subunit, a trans C^8−N^9 *N*-methyl amide central to a typical type II β-turn capped with a tight transannular Ala[1]-C=O-HN-Ala[4] hydrogen bond, a trans C^{14}−N^{15} *N*-methyl amide, and a fully accessible Ala[2]-NH. Unlike the conformation observed in THF-d_8 but similar to the X-ray structure conformation, the LiCl complexed conformation of RA-VII lacks the weak transannular Ala[1]-NH-O=C-Ala[4] hydrogen bond which results in a small perturbation in the relative orientations of the two aromatic rings of the characteristic biaryl ether ring system. This may be attributed to preferential complexation or a preferential effect of the LiCl complexation to the Ala[1]-Tyr[6] amide. Interestingly, and not fortuitous, this is the exact location occupied by an ordered water molecule in the X-ray crystal structure of a derivative of RA-VII. The differences with the LiCl complexed agent or the X-ray conformation and the major conformation observed in THF-d_8 are small and constitute subtle conformational changes in the backbone orientation suggesting that this single dominant conformation represents the relevant physiological conformation in water as well. In contrast, the 14-membered cycloisodityrosine **9** adopts a rigid conformation possessing a trans *N*-methyl amide central to its structure which is unaffected by LiCl complexation. Thus, its adoption of an inherently disfavored cis amide central to its structure within the bicyclic hexapeptide of the natural products is not solvent induced or solvent dependent.

Bouvardin[1] and deoxybouvardin,[1] bicyclic hexapeptides isolated from *Bouvardia ternifolia* (Rubiaceae), represent the initial members of a growing class of potent antitumor antibiotics now including *O*-methyl bouvardin[1] and RA-I−RA-XIV (Figure 1).[2−5] Both RA-VII (**1**) and bouvardin (**3**) inhibit protein synthesis[6] through binding to eukaryotic 80S ribosomes[6,7] with inhibition of both amino acyl *t*RNA binding and peptidyl *t*RNA translocation[6−9] and this is presently thought to be the site of

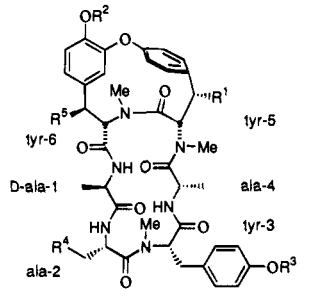

	R[1]	R[2]	R[3]	R[4]	R[5]	
1	H	Me	Me	H	H	RA-VII
2	H	H	Me	H	H	RA-V, deoxybouvardin
3	OH	H	Me	H	H	bouvardin
4	H	H	Me	OH	H	RA-I
5	H	Me	H	H	H	RA-II
6	H	Me	Me	OH	H	RA-III
7	H	Me	Me	H	OH	RA-IV
8	OH	Me	Me	H	H	6-*O*-methylbouvardin

Figure 1.

[⊗] Abstract published in *Advance ACS Abstracts*, July 1, 1995.

(1) Jolad, S. D.; Hoffmann, J. J.; Torrance, S. J.; Wiedhopf, R. M.; Cole, J. R.; Arora, S. K.; Bates, R. B.; Gargiulo, R. L.; Kriek, G. R. *J. Am. Chem. Soc.* **1977**, *99*, 8040. Bates, R. B.; Cole, J. R.; Hoffmann, J. J.; Kriek, G. R.; Linz, G. S.; Torrance, S. J. *J. Am. Chem. Soc.* **1983**, *105*, 1343.

(2) Itokawa, H.; Takeya, K. *Heterocycles* **1993**, *35*, 1467.

(3) Itokawa, H.; Takeya, K.; Mori, N.; Sonobe, T.; Mihashi, S.; Hamanaka, T. *Chem. Pharm. Bull.* **1986**, *34*, 3762. Itokawa, H.; Takeya, K.; Mihara, K.; Mori, N.; Hamanaka, T.; Sonobe, T.; Iitaka, Y. *Chem. Pharm. Bull.* **1983**, *31*, 1424. Itokawa, H.; Takeya, K.; Mori, N.; Kidokoro, S.; Yamamoto, H. *Planta Med.* **1984**, *51*, 313. Itokawa, H.; Takeya, K.; Mori, N.; Hamanaka, T.; Sonobe, T.; Mihara, K. *Chem. Pharm. Bull.* **1984**, *32*, 284. Itokawa, H.; Takeya, K.; Mori, N.; Sonobe, T.; Serisawa, N.; Hamanaka, T.; Mihashi, S. *Chem. Pharm. Bull.* **1984**, *32*, 3216. Itokawa, H.; Takeya, K.; Mori, N.; Takanashi, M.; Yamamoto, H.; Sonobe, T.; Kidokoro, S. *Gann* **1984**, *75*, 929. Morita, H.; Yamamiya, T.; Takeya, K.; Itokawa, H. *Chem. Pharm. Bull.* **1992**, *40*, 1352.

(4) Morita, H.; Kondo, K.; Hitotsuyanagi, Y.; Takeya, K.; Itokawa, H.; Tomioka, N.; Itai, A.; Iitaka, Y. *Tetrahedron* **1991**, *47*, 2757. Itokawa, H.; Morita, H.; Takeya, K.; Tomioka, N.; Itai, A. *Chem. Lett.* **1991**, 2217. Itokawa, H.; Yamamiya, T.; Morita, H.; Takeya, K. *J. Chem. Soc., Perkin Trans. 1* **1992**, 455. Itokawa, H.; Morita, H.; Takeya, K.; Tomioka, N.; Itai, A.; Iitaka, Y. *Tetrahedron* **1991**, *47*, 7007. Itokawa, H.; Morita, H.; Takeya, K. *Chem. Pharm. Bull.* **1992**, *40*, 1050. Itokawa, H.; Saitou, K.; Morita, H.; Takeya, K.; Yamada, K. *Chem. Pharm. Bull.* **1992**, *40*, 2984. Itokawa, H.; Suzuki, J.; Hitotsuyanagi, Y.; Kondo, K.; Takeya, K. *Chem. Lett.* **1993**, *42*, 1402. Itokawa, H.; Kondo, K.; Hitotsuyanagi, Y.; Isomura, M.; Takeya, K. *Chem. Pharm. Bull.* **1993**, *42*, 1402. Hitotsuyanagi, Y.; Suzuki, J.; Takeya, K.; Itokawa, H. *Bioorg. Med. Chem. Lett.* **1994**, *4*, 1633.

(5) Itokawa, H.; Saitou, K.; Morita, H.; Takeya, K. *Chem. Pharm. Bull.* **1991**, *39*, 2161.

(6) Tobey, R. A.; Orlicky, D. J.; Deaven, L. L.; Rall, L. B.; Kissane, R. J. *Cancer Res.* **1978**, *38*, 4415.

(7) Marita, H.; Yamamiya, T.; Takeya, K.; Itokawa, H.; Sakuma, C.; Yamada, J.; Suga, T. *Chem. Pharm. Bull.* **1993**, *41*, 781.

0002-7863/95/1517-7357$09.00/0

action for the agent antitumor activity.[10] The examination of the structures **1**−**3** led to the initial proposal that the cycloisodityrosine derived 14-membered ring may serve the scaffolding role of inducing and maintaining a rigid, normally inaccessible conformation within the biologically active tetrapeptide housed in the 18-membered ring and that it was the strained conformational constraints of the cycloisodityrosine subunit that forced its adoption of a cis *N*-methyl amide central to its structure.[1] However, more recent studies have identified the cycloisodityrosine subunit as the pharmacophore and have led to the reversal of these assigned functional roles.[11−20] These studies have shown that it is the tetrapeptide housed in the 18-membered ring which induces and maintains the rigid, normally inaccessible cis amide conformation within the biologically active 14-membered cycloisodityrosine subunit.[11−20]

The X-ray crystal structure of bouvardin (**3**)[1] and a derivative of deoxybouvardin (**2**)[4] revealed that the agents adopt a conformation in which the three secondary amides and the C^8−N^9 and C^{14}−N^{15} *N*-methyl amides in the 18-membered ring possess the trans stereochemistry, while the C^{30}−N^{29} *N*-methyl amide central to the cycloisodityrosine 14-membered ring adopts the cis amide stereochemistry. Similarly, the conformational properties of members of **1**−**8** and related analogs[1,4,5,11−21] have been studied by ^{1}H NMR in a range of conventional solvents ($CDCl_3$, CD_3OD, DMSO-d_6). Depending on the solvent, **1**−**3** have each been shown to adopt a single predominant solution conformation that closely resembles the X-ray structure conformation. For RA-VII, the major conformation has been shown to constitute 88% ($CDCl_3$), 83% (15% CD_3OD−$CDCl_3$), and 64% (DMSO-d_6) of the mixture.[20] However, an additional minor conformation for the agent is always observed and has been unambiguously determined to possess both a C^{30}−N^{29} and C^8−N^9 cis amide.[20] This minor conformation has been shown to constitute 12% ($CDCl_3$), 17% (15% CD_3OD−$CDCl_3$), and 32% (DMSO-d_6) of the mixture.[20] An additional trace conformational isomer thought to constitute the C^{30}−N^{29}, C^8−N^9, and C^{14}−N^{15} cis amide isomer has been occasionally detected (4% in DMSO-d_6).[4,20]

Although the conformation of cyclic peptides in water may be substantially different from that observed in nonpolar or aprotic solvents as well as different from that observed in the solid state, a direct correlation between adoption of a conformation possessing a cis C^{30}−N^{29} amide and the observation of biological activity has been observed with analogs of RA-VII suggesting that the major conformational isomer of the natural products is biologically relevant.[20] Moreover, the enhancement of biological potency observed with the removal of the N^9-methyl group of **3** which restricts the resulting agent exclusively to this single conformation in all conventional NMR solvents ($CDCl_3$, CD_3OD, DMSO-d_6) has supported the expectation that this may be biologically relevant.[19] Consequently, in conjunction with these studies we have been interested in assessing the conformational properties of the agents in water. However, the solubility of the agents in water is too low for a conformational analysis to be carried out.

Herein, we report the ^{1}H NMR studies of RA-VII in THF-d_8 and in THF-d_8 with added LiCl. The addition of lithium salts to THF has been shown to affect the solubility,[22] promote deaggregation,[23] and alter the conformational properties of peptides.[24−26] Notably, the LiCl complexed cyclic peptides have been suggested to more accurately reflect the conformational properties in water than those obtained in conventional solvents alone. For example, cyclosporin A adopts a conformation that contains the correct amide stereochemistries found in the bound conformation in the CsA−cyclophilin complex[25,26] and binds to the protein without kinetic barriers due to conformational interconversion in the presence of LiCl.[26] Thus, the LiCl−THF solution conformation of cyclic peptides may more closely reflect the native conformation(s) in water and might be expected to do so by disrupting intramolecular and intermolecular hydrogen bonds necessarily adopted in nonpolar or aprotic solvents.

The addition of LiCl to solutions of RA-VII in THF-d_8 resulted in the shift of the conformational equilibria to essentially a single conformation. The minor conformational isomers detected in THF-d_8 were converted to essentially a single conformational isomer that closely resembles the X-ray crystal and major solution conformation observed in the absence of LiCl. Like the X-ray and conventional solution conformation, this LiCl complexed conformation possesses the unusual type IV β-turn and characteristic central cis C^{30}−N^{29} amide and more conventional type II β-turn and typical central trans C^8−N^9 amide. Unlike the conventional solution conformation but like the X-ray structure conformation, the LiCl complexed conformation lacks the weak transannular Ala^1-NH-O=C-Ala^4 hydrogen bond but maintains the Ala^1-C=O-HN-Ala^4 hydrogen bond capping the typical type II β-turn.

^{1}H NMR of RA-VII in THF-d_8. The ^{1}H NMR of RA-VII (**1**) in THF-d_8 was recorded and fully assigned through use of

(8) Johnson, R. K.; Chitnis, M. P. *Proc. Am. Assoc. Cancer Res.* **1978**, *19*, 218. Chitnis, M. P.; Alate, A. D.; Menon, R. S. *Chemotherapy (Basel)* **1981**, *27*, 126. Chitnis, M.; Menon, R.; Adwankar, M.; Satyamoorthy, K. *Tumori* **1985**, *71*, 261. Chitnis, M. P.; Adwankar, M. K. *J. Cancer Res. Clin. Oncol.* **1986**, *112*, 131.

(9) Zalacain, M.; Zaera, E.; Vazquez, D.; Jiminez, A. *FEBS Lett.* **1982**, *148*, 95.

(10) Hamanaka, T.; Ohgoshi, M.; Kawahara, K.; Yamakawa, K.; Tsuruo, T.; Tsukagoshi, S. *J. Pharmacobio-Dyn.* **1987**, *10*, 616. Kato, T.; Suzumura, Y.; Takamoto, S.; Ota, K. *Anticancer Res.* **1987**, *7*, 329. Majima, H.; Tsukagoshi, S.; Furue, H.; Suminaga, M.; Sakamoto, K.; Wakabayashi, R.; Kishino, S.; Niitani, H.; Murata, A.; Genma, A.; Nukariya, N.; Uematsu, K.; Furuta, T.; Kurihara, M.; Yoshida, F.; Isomura, S.; Takemoto, T.; Hirashima, M.; Izumi, T.; Nakao, I.; Ohashi, Y.; Ito, K.; Asai, R. *Jpn. J. Cancer Chemother.* **1993**, *20*, 67.

(11) Boger, D. L.; Myers, J. B.; Yohannes, D.; Kitos, P. A.; Suntornwat, O.; Kitos, J. C. *Bioorg. Med. Chem. Lett.* **1991**, *1*, 313.

(12) Boger, D. L.; Yohannes, D.; Myers, J. B. *J. Org. Chem.* **1992**, *57*, 1319.

(13) Boger, D. L.; Yohannes, D.; Zhou, J.; Patane, M. A. *J. Am. Chem. Soc.* **1993**, *115*, 3420. Boger, D. L.; Yohannes, D. *J. Am. Chem. Soc.* **1991**, *113*, 1427. Boger, D. L.; Yohannes, D. *J. Org. Chem.* **1991**, *56*, 1763.

(14) Boger, D. L.; Patane, M. A.; Jin, Q.; Kitos, P. A. *Bioorg. Med. Chem.* **1994**, *2*, 85. Boger, D. L.; Zhou, J. *J. Am. Chem. Soc.* **1993**, *115*, 11426.

(15) Boger, D. L.; Yohannes, D. *J. Org. Chem.* **1988**, *53*, 487. Bates, R. B.; Gin, S. L.; Hassen, M. A.; Hruby, V. J.; Janda, K. D.; Kriek, G. R.; Michaud, J.-P.; Vine, D. B. *Heterocycles* **1984**, *22*, 785.

(16) Boger, D. L.; Yohannes, D. *Synlett* **1990**, *1*, 33.

(17) Boger, D. L.; Myers, J. B. *J. Org. Chem.* **1991**, *56*, 5385.

(18) Boger, D. L.; Yohannes, D. *Bioorg. Med. Chem. Lett.* **1993**, *3*, 245.

(19) Boger, D. L.; Patane, M. A.; Zhou, J. *J. Am. Chem. Soc.* **1994**, *116*, 8544.

(20) Boger, D. L.; Zhou, J. *J. Am. Chem. Soc.* **1995**, *117*, 7364 (following paper in this issue).

(21) Senn, H.; Loosli, H.-R.; Sanner, M.; Braun, W. *Biopolymers* **1990**, *29*, 1387.

(22) Seebach, D.; Thaler, A.; Beck, A. K. *Helv. Chim. Acta* **1989**, *72*, 857.

(23) Thaler, A.; Seebach, D.; Cardinaux, F. *Helv. Chim. Acta* **1991**, *74*, 617, 628.

(24) Kessler, H.; Hehlein, W.; Schuck, R. *J. Am. Chem. Soc.* **1982**, *104*, 4534.

(25) Kock, M.; Kessler, H.; Seebach, D.; Thaler, A. *J. Am. Chem. Soc.* **1992**, *114*, 2676. Seebach, D.; Beck, A. K.; Bossler, H. G.; Gerber, C.; Ko, S. Y.; Murtiashaw, C. W.; Naef, R.; Shoda, S.; Thaler, A.; Krieger, M.; Wenger, R. *Helv. Chim. Acta* **1993**, *76*, 1564. Seebach, D.; Bossler, H. G.; Flowers, R.; Arnett, E. M. *Helv. Chim. Acta* **1994**, *77*, 291. Review: Seebach, D.; Beck, A. K.; Studer, A. In *Modern Synthetic Methods*; Ernst, B., Leumann, C., eds.; VCH Publishers: Weinheim, 1995; pp 3−178.

(26) Kofron, J. L.; Kuzmic, P.; Kishore, V.; Gemmecker, G.; Fesik, S. W.; Rich, D. H. *J. Am. Chem. Soc.* **1992**, *114*, 2670.

Table 1. ^{1}H NMR Assignments For RA-VII (THF-d_8)[a]

proton	chemical shift (δ)	decoupling result
Ala$^{4\beta}$	1.03 (3H, d, J = 6.6 Hz)	4.68 dq→d
Ala$^{1\beta}$	1.17 (3H, d, J = 7.0 Hz)	4.37 dq→d
Ala$^{2\beta}$	1.25 (3H, d, J = 6.8 Hz)	4.78 dq→d
Tyr$^{5\beta a}$	2.56 (1H, dd, J = 3.1, 11.2 Hz)	5.47 dd→d/3.60 dd→d
Tyr^6-NCH$_3$	2.63 (3H, s)	
Tyr^3-NCH$_3$	2.90 (3H, s)	
Tyr$^{6\beta a,b}$	3.00 (2H, m)	4.58 dd→s
Tyr^5-NCH$_3$	3.04 (3H, s)	
Tyr$^{3\beta a}$	3.23 (1H, dd, J = 4.8, 13.8 Hz)	3.59 dd→d/3.32 dd→d
Tyr$^{3\beta b}$	3.32 (1H, dd, J = 10.8, 13.8 Hz),	3.59 dd→d/3.23 dd→d
Tyr$^{3\alpha}$	3.59 (1H, dd, J = 4.8, 10.8 Hz)	3.32 dd→d/3.23 dd→d
Tyr$^{5\beta b}$	3.60 (1H, dd, J = 11.2, 11.3 Hz)	5.47 dd→d/2.56 dd→d
Tyr^3-OCH$_3$	3.74 (3H, s)	
Tyr^6-OCH$_3$	3.84 (3H, s)	
Ala$^{1\alpha}$	4.37 (1H, dq, J = 6.8, 7.0 Hz)	7.23 d→s/1.17 d→s
Tyr$^{6\delta b}$	4.55 (1H, d, J = 2.2 Hz)	6.57 dd→d
Tyr$^{6\alpha}$	4.58 (1H, dd, J = 4.6, 11.1 Hz)	3.00 m→d
Ala$^{4\alpha}$	4.68 (1H, dq, J = 6.6, 7.8 Hz)	6.64 d→s/1.03 d→s
Ala$^{2\alpha}$	4.78 (1H, dq, J = 6.8, 8.4 Hz)	7.81 d→s/1.25 d→s
Tyr$^{5\alpha}$	5.47 (1H, dd, J = 3.1, 11.3 Hz)	3.60 dd→d/2.56 dd→d
Tyr$^{6\delta a}$	6.57 (1H, dd, J = 2.2, 8.3 Hz)	6.81 d→s/4.55 d→s
Ala^4-NH	6.64 (1H, d, J = 7.8 Hz)	4.68 dq→q
Tyr$^{5\epsilon b}$	6.75 (1H, dd, J = 2.4, 8.4 Hz)	7.21 dd→d/7.14 dd→d
Tyr$^{6\epsilon a}$	6.81 (1H, d, J = 8.3 Hz)	6.57 dd→d
Tyr$^{3\epsilon}$	6.82 (2H, d, J = 8.6 Hz)	7.05 d→s
Tyr$^{3\delta}$	7.05 (2H, d, J = 8.6 Hz)	6.82 d→s
Try$^{5\epsilon a}$	7.14 (1H, dd, J = 2.4, 8.2 Hz)	7.36 dd→d/6.75 dd→d
Tyr$^{5\delta b}$	7.21 (1H, dd, J = 2.2, 8.4 Hz)	7.36 dd→d/6.75 dd→d
Ala^1-NH	7.23 (1H, d, J = 6.8 Hz)	4.37 dq→q
Tyr$^{5\delta a}$	7.36 (1H, dd, J = 2.2, 8.2 Hz)	7.21 dd→d/7.14 dd→d
Ala^2-NH	7.81 (1H, d, J = 8.4 Hz)	4.78 dq→q

[a] Major conformational isomer.

decoupling, ^{1}H−^{1}H NOESY and ROESY NMR experiments (Tables 1 and 2). The ROESY spectrum was used to distinguish NOE and exchange peaks and the distinguishable sets of signals obtained in the 1D ^{1}H NMR spectrum were confirmed as conformational isomers. The spectral properties of **1** in THF-d_8 were analogous to those observed in other solvents, and it exhibited the same conformational equilibria observed previously (Table 1). Three distinct conformations were detected in a ratio of 78:20:2 (Figure 2). The major conformation closely approximates the X-ray structure conformation and contains a cis C^{30}−N^{29} *N*-methyl amide and trans C^8−N^9 and C^{14}−N^{15} *N*-methyl amides. Characteristic and diagnostic of the cis C^{30}−N^{29} *N*-methyl amide central to a type VI β-turn, an intense NOE was observed between Tyr$^{5\alpha}$-H/Tyr$^{6\alpha}$-H. Similarly, no NOE was observed between Tyr$^{5\alpha}$-H or Tyr$^{6\alpha}$-H and Tyr^6-NCH$_3$ which would be diagnostic of a trans C^{30}−N^{29} *N*-methyl amide. Diagnostic of a trans C^8−N^9 *N*-methyl amide central to a type II β-turn, both an Ala$^{2\alpha}$-H/Tyr^3-NCH$_3$ and Tyr$^{3\alpha}$-H/Tyr^3-NCH$_3$ strong NOE were observed, and no Ala$^{2\alpha}$-H/Tyr$^{3\alpha}$-H NOE was detected which would be characteristic of a cis C^8−N^9 *N*-methyl amide. Characteristic of the orientation and stereochemistry of the trans C^{14}−N^{15} *N*-methyl amide, NOEs between Tyr^5-NCH$_3$ and Ala$^{4\alpha}$-H and Ala$^{4\beta}$-H were observed, while that of Tyr$^{5\alpha}$-H/Tyr^5-NCH$_3$ was not, and no NOE for Tyr$^{5\alpha}$-H/Ala$^{4\alpha}$-H was observed which would be diagnostic of a cis C^{14}−N^{15} amide.

The minor conformation contains both a cis C^{30}−N^{29} and C^8−N^9 *N*-methyl amide and a trans C^{14}−N^{15} *N*-methyl amide. In this conformation, diagnostic Tyr$^{6\alpha}$-H/Tyr$^{5\alpha}$-H, Ala$^{2\alpha}$-H/Tyr$^{3\alpha}$-H, Tyr^5-NCH$_3$/Ala$^{4\alpha}$-H, and Tyr^5-NCH$_3$/Ala$^{4\beta}$-H NOE were observed. Aside from the differences about the C^8−N^9 amide in the 1D and 2D ^{1}H NMR, the major and minor conformations of RA-VII were otherwise the same indicating that the sole difference in the two conformations is cis−trans isomerization about the C^8−N^9 *N*-methyl amide. The third trace conformation detected was not assigned but in analogy to prior

Table 2. ^{1}H−^{1}H NOE Observed with RA-VII in THF-d_8[a]

crosspeak	chemical shift (δ)
Ala^2-NH/Ala$^{2\alpha}$	7.81/4.78
Ala^2-NH/Ala$^{1\alpha}$	7.81/4.37
Ala^2-NH/Ala$^{2\beta}$	7.81/1.25
Ala^2-NH/Ala$^{1\beta}$	7.81/1.17
Tyr$^{5\delta a}$/Tyr$^{5\epsilon a}$	7.36/7.14
Tyr$^{5\delta a}$/Tyr$^{5\alpha}$	7.36/5.47
Tyr$^{5\delta a}$/Tyr$^{5\beta a}$	7.36/2.56
Ala^1-NH/Tyr$^{6\alpha}$	7.23/4.58
Ala^1-NH/Ala$^{1\beta}$	7.23/1.17
Tyr$^{5\delta b}$/Tyr$^{5\epsilon b}$	7.21/6.75
Tyr$^{5\delta b}$/Tyr$^{5\beta b}$	7.21/3.60
Tyr$^{5\epsilon a}$/Tyr$^{6\delta b}$	7.14/4.55
Tyr$^{3\delta}$/Tyr$^{3\epsilon}$	7.05/6.82
Tyr$^{3\delta}$/Tyr$^{3\alpha}$	7.05/3.59
Tyr$^{3\delta}$/Tyr$^{3\beta b}$	7.05/3.32
Tyr$^{3\delta}$/Tyr$^{3\beta a}$	7.05/3.23
Tyr$^{3\epsilon}$/Tyr^3-OCH$_3$	6.82/3.74
Tyr$^{6\epsilon a}$/Tyr$^{6\delta a}$	6.81/6.57
Tyr$^{6\epsilon a}$/Tyr^6-OCH$_3$	6.81/3.84
Ala^4-NH/Ala$^{4\alpha}$	6.64/4.68
Ala^4-NH/Tyr$^{3\alpha}$	6.64/3.59
Ala^4-NH/Tyr^3-NCH$_3$	6.64/2.90
Ala^4-NH/Ala$^{4\beta}$	6.64/1.03
Tyr$^{6\delta a}$/Tyr$^{6\beta a}$	6.57/3.00
Tyr$^{5\alpha}$/Ala$^{6\alpha}$	5.47/4.58
Tyr$^{5\alpha}$/Tyr$^{5\beta b}$	5.47/3.60
Tyr$^{5\alpha}$/Tyr$^{5\beta a}$	5.47/2.56
Ala$^{2\alpha}$/Tyr^3-NCH$_3$	4.78/2.90
Ala$^{2\alpha}$/Ala$^{2\beta}$	4.78/1.25
Ala$^{4\alpha}$/Tyr^5-NCH$_3$	4.68/3.04
Ala$^{4\alpha}$/Ala$^{4\beta}$	4.68/1.03
Tyr$^{6\alpha}$/Tyr$^{6\delta b}$	4.58/4.55
Tyr$^{6\alpha}$/Tyr$^{6\beta a}$	4.58/3.00
Ala$^{1\alpha}$/Ala$^{1\beta}$	4.37/1.17
Ala$^{1\alpha}$/Ala$^{4\beta}$	4.37/1.03
Tyr$^{5\beta b}$/Tyr^6-NCH$_3$	3.60/2.63
Tyr$^{5\beta b}$/Tyr$^{5\beta a}$	3.60/2.56
Tyr$^{3\alpha}$/Tyr$^{3\beta b}$	3.59/3.32
Tyr$^{3\alpha}$/Tyr$^{3\beta a}$	3.59/3.23
Tyr$^{3\alpha}$/Tyr^3-NCH$_3$	3.59/2.90
Tyr$^{3\beta b}$/Tyr$^{3\beta a}$	3.32/3.23
Tyr^5-NCH$_3$/Ala$^{4\beta}$	3.04/1.03
Tyr$^{6\delta b}$/Tyr^6-NCH$_3$	3.00/2.63

[a] Major conformational isomer.

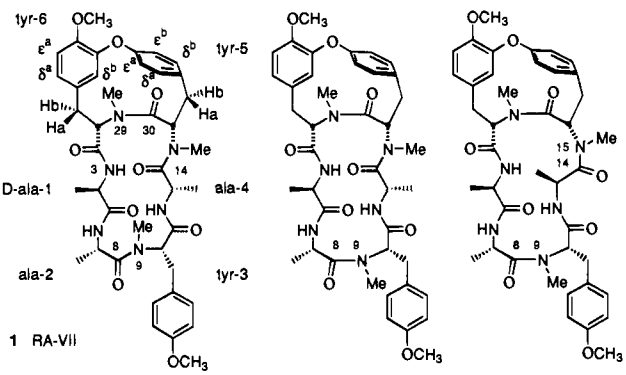

	ctt	cct	ccc
$CDCl_3$:	88	12	-
15% CD_3OD-$CDCl_3$:	83	17	-
DMSO-d_6:	64	32	4
THF-d_8:	78	20	2
THF-d_8/LiCl:	94	6	-

Figure 2.

studies in DMSO-d_6 might be expected to represent the all cis *N*-methyl amide conformation.[4]

^{1}H NMR of RA-VII Complexed with LiCl in THF-d_8. The addition of 1.0 equiv of LiCl to a sample of RA-VII (**1**) in THF-

Table 3. ^{1}H NMR Assignments for Lithium Chloride Complexed RA-VII in THF-d_8

proton		chemical shift, δ (multiplicity, J =)		
		1.0 equiv LiCl	2.0 equiv LiCl	12.0 equiv LiCl
Ala$^{4\beta}$	3H	1.02 (d, 6.7)	1.03 (d, 6.7)	1.10 (d, 6.8)
Ala$^{1\beta}$	3H	1.28 (d, 7.5)	1.30 (d, 7.4)	1.37 (d, 7.1)
Ala$^{2\beta}$	3H	1.30 (d, 7.8)	1.32 (d, 7.2)	1.41 (d, 7.0)
Tyr$^{5\beta a}$	1H	2.56 (dd, 2.7, 11.3)	2.59 (dd, 2.7, 11.3)	2.69 (dd, 2.8, 11.2)
Tyr^6-NCH$_3$	3H	2.60 (s)	2.60 (s)	2.62 (s)
Tyr^3-NCH$_3$	3H	2.84 (s)	2.81 (s)	2.92 (s)
Tyr$^{6\beta b}$	1H	2.84 (dd, 3.2, 19.0)	2.81 (m)	2.87 (m)
Tyr^5-NCH$_3$	3H	3.04 (s)	3.05 (s)	3.14 (s)
Tyr$^{6\beta a}$	1H	3.09 (dd, 11.0, 19.0)	3.10 (m)	3.12 (m)
Tyr$^{3\beta b}$	1H	3.28 (dd, 9.0, 9.0)	3.27 (dd, 10.0, 10.0)	3.33 (br s)
Tyr$^{3\beta a}$	1H	3.28 (dd, 6.7, 9.0)	3.27 (dd, 6.1, 10.0)	3.33 (br s)
Tyr$^{5\beta b}$	1H	3.49 (t, 11.3)	3.48 (t, 11.3)	3.53 (t, 11.2)
Tyr$^{3\alpha}$	1H	3.68 (dd, 6.7, 9.0)	3.71 (dd, 6.1, 10.0)	4.04 (dd, 5.4, 10.4)
Tyr^3-OCH$_3$	3H	3.73 (s)	3.73 (s)	3.74 (s)
Tyr^6-OCH$_3$	3H	3.86 (s)	3.87 (s)	3.85 (s)
Ala$^{2\alpha}$	1H	4.62 (dq, 6.8, 7.8)	4.61 (dq, 6.6, 7.2)	4.65 (dq, 6.6, 7.0)
Ala$^{1\alpha}$	1H	4.69 (dq, 7.5, 7.6)	4.74 (dq, 7.4, 7.7)	4.94 (dq, 7.1, 9.7)
Ala$^{4\alpha}$	1H	4.85 (dq, 6.7, 8.5)	4.87 (dq, 6.7, 8.4)	5.09 (dq, 6.8, 7.9)
Tyr$^{6\delta b}$	1H	5.21 (br s)	5.24 (br s)	5.13 (br s)
Tyr$^{6\alpha}$	1H	5.38 (dd, 3.2, 11.0)	5.42 (dd, 3.6, 11.8)	5.46 (dd, 3.7, 11.7)
Tyr$^{5\alpha}$	1H	5.60 (dd, 2.7, 11.3)	5.60 (dd, 3.7, 11.3)	5.58 (dd, 2.8, 11.2)
Tyr$^{6\delta a}$	1H	6.52 (dd, 1.8, 8.2)	6.52 (dd, 1.8, 8.3)	6.54 (dd, 2.0, 8.3)
Ala^4-NH	1H	6.56 (d, 8.5)	6.59 (d, 8.4)	6.89 (d, 7.9)
Tyr$^{5\epsilon b}$	1H	6.60 (dd, 2.4, 8.4)	6.58 (dd, 2.4, 8.5)	6.58 (dd, 2.4, 8.4)
Tyr$^{6\epsilon a}$	1H	6.78 (d, 8.2)	6.78 (d, 8.3)	6.76 (d, 8.3)
Tyr$^{3\epsilon}$	2H	6.81 (d, 8.6)	6.81 (d, 8.6)	6.79 (d, 8.6)
Tyr$^{3\delta}$	2H	7.06 (d, 8.6)	7.07 (d, 8.6)	7.19 (d, 8.6)
Tyr$^{5\delta b}$	1H	7.10 (dd, 2.2, 8.4)	7.10 (dd, 2.1, 8.5)	7.16 (dd, 1.8, 8.4)
Tyr$^{5\epsilon a}$	1H	7.35 (dd, 2.4, 8.2)	7.36 (dd, 2.4, 8.2)	7.35 (dd, 2.4, 8.3)
Tyr$^{5\delta a}$	1H	7.56 (dd, 2.2, 8.2)	7.58 (dd, 2.1, 8.2)	7.68 (dd, 2.0, 8.3)
Ala^2-NH	1H	8.68 (d, 6.8)	8.97 (d, 6.6)	9.80 (d, 6.6)
Ala^1-NH	1H	8.73 (d, 7.6)	8.78 (d, 7.7)	8.89 (d, 9.7)

d_8 resulted in the coalescence to one major conformation detectable by ^{1}H NMR with only trace amounts of the second isomer present in a ratio of 94:6. In addition, several large chemical shifts were observed (Table 3). As detailed below, this predominant conformation observed in LiCl−THF-d_8 maintained the seminal elements of the major conformation observed in THF-d_8 alone and contains a cis C^{30}−N^{29} *N*-methyl amide and trans C^8−N^9 and C^{14}−N^{15} *N*-methyl amides. As detailed above for the major conformation detected in THF-d_8 alone, a characteristic and intense NOE was observed for Tyr$^{6\alpha}$-H/Tyr$^{5\alpha}$-H diagnostic of a cis C^{30}−N^{29} *N*-methyl amide, and no NOE was detected between Tyr$^{5\alpha}$-H or Tyr$^{6\alpha}$-H and Tyr^6-NCH$_3$ which would be diagnostic of a trans C^{30}−N^{29} *N*-methyl amide. Similarly, the NOE characteristic of trans C^8−N^9 and C^{14}−N^{15} *N*-methyl amides were evident including Ala$^{2\alpha}$-H/Tyr^3-NCH$_3$, Tyr$^{3\alpha}$-H/Tyr^3-NCH$_3$, Ala$^{4\alpha}$-H/Tyr^5-NCH$_3$, and Ala$^{4\beta}$-H/Tyr^5-NCH$_3$, and those characteristic of a cis *N*-methyl amide were not detected, Ala$^{2\alpha}$-H/Tyr$^{3\alpha}$-H and Tyr$^{5\alpha}$-H/Ala$^{4\alpha}$-H.

The addition of a second equivalent of LiCl resulted in little change in the conformational ratio, but a larger effect on the perturbed chemical shifts was observed (Tables 3 and 4). The addition of 10 more equiv of LiCl caused little further change in the ^{1}H NMR spectrum (Tables 3 and 4).

Characteristic of an amide NH involved in tight hydrogen bonding and capping a type II β-turn, the Ala^4-NH exchanges very slowly ($t_{1/2}$ > 2 days) and exhibits little or no chemical shift solvent dependence. Similarly, the addition of 1 or 2 equiv of LiCl had no effect on the Ala^4-NH chemical shift indicating that the structure of this tight type II β-turn hydrogen bond between Ala^4-NH-O=C-Ala^1 is not disrupted (Table 4). In contrast, Ala^2-NH exchanges very rapidly ($t_{1/2}$ < 30 min), experiences the widest range of chemical shift solvent dependence, may be selectively alkylated,[3,4] and thus is considered completely accessible and not engaged in hydrogen bonding. Consistent with this conclusion, the Ala^2-NH experiences a large increase in chemical shift (0.9−1.2 ppm) upon LiCl complexation (Table 4). The Ala^1-NH exhibits an intermittent exchange rate ($t_{1/2} \leq 10$ h), exhibits a more modest chemical shift solvent dependency, and is not alkylated as readily as Ala^2-NH. Thus, it has been considered to be involved in weak hydrogen bonding. Consistent with this, the Ala^1-NH exhibits the largest chemical shift increase (1.5−2.5 ppm) upon LiCl complexation indicative of disruption of a weak or long distant Ala^1-NH-O=C-Ala^4 hydrogen bond (Table 4). Upon addition of 1.0 equiv of LiCl, both Ala^1-NH and Ala^2-NH exhibit the same chemical shift (δ 8.73 and 8.68) indicative of comparable solvent exposure, and the Ala^1-NH experienced a 1.50 ppm shift versus 0.87 ppm for the Ala^2-NH while that of Ala^4-NH is unperturbed at δ 6.54.

This suggests that the LiCl complexation occurs preferentially at the Ala^1 amide or that a conformational effect of the complexation of 1.0 equiv of LiCl is perceptible only with complexation to the Ala^1 amide. Consistent with this observation, the remaining significant chemical shift perturbations are centered about the Ala^1 residue and the adjacent Tyr^6 residue. Interestingly, this is the exact location of an ordered water molecule located in the X-ray crystal structure of a derivative of **1** and **2**.[4] Little or no changes in the Ala^2 (except the Ala^2-NH), Tyr^3, Ala^4, or Tyr^5 residues were experienced except for small changes in the Tyr^5 aromatic hydrogen chemical shifts indicative of a small conformational change in the relative orientations of the two aromatic rings of the Tyr^5−Tyr^6 biaryl ether. Upon complexation with 1.0 equiv LiCl, the Ala$^{1\alpha}$-H suffers a 0.32 ppm downfield shift and the Tyr$^{6\alpha}$-H suffers a larger 0.8 ppm downfield shift, and little further change is experienced upon addition of more LiCl. Analogous to the location of an ordered water molecule in the X-ray structure of **1**,[4] this suggests that the lithium cation is complexed to the Ala^1 carbonyl oxygen in the plane of the amide and preferentially

Table 4. Comparison of ^{1}H NMR Chemical Shifts of RA-VII and Lithium Chloride Complexed RA-VII in THF-d_8[a]

amino acid	proton	0.0 equiv LiCl	1.0 equiv LiCl	2.0 equiv LiCl	12.0 equiv LiCl
D-Ala-1	Hα	4.37	4.69	4.74	4.94
	Hβ	1.17	1.28	1.30	1.37
	H_N	7.23	8.73	8.78	8.89
Ala-2	Hα	4.78	4.62	4.61	4.65
	Hβ	1.25	1.30	1.32	1.41
	H_N	7.81	8.68	8.97	9.80
Tyr-3	Hα	3.59	3.68	3.71	4.04
	Hβa	3.23	3.29	3.27	3.33
	Hβb	3.32	3.27	3.27	3.33
	2Hδ	7.05	7.06	7.07	7.19
	2Hε	6.82	6.81	6.81	6.79
	CH_3N	2.90	2.84	2.81	2.92
	CH_3O	3.74	3.73	3.73	3.74
Ala-4	Hα	4.68	4.85	4.87	5.09
	Hβ	1.03	1.02	1.03	1.10
	H_N	6.64	6.56	6.59	6.89
Tyr-5	Hα	5.47	5.60	5.60	5.58
	Hβa	2.56	2.56	2.59	2.69
	Hβb	3.60	3.49	3.48	3.53
	Hδa	7.36	7.56	7.58	7.68
	Hδb	7.21	7.10	7.10	7.16
	Hεa	7.14	7.35	7.36	7.35
	Hεb	6.75	6.60	6.58	6.58
	CH_3N	3.04	3.04	3.05	3.14
Tyr-6	Hα	4.58	5.38	5.42	5.46
	Hβa	3.00	3.09	3.10	3.12
	Hβb	3.00	2.84	2.81	2.67
	Hδa	6.57	6.52	6.52	6.54
	Hδb	4.55	5.21	5.24	5.13
	Hεa	6.81	6.78	6.78	6.76
	CH_3N	2.63	2.60	2.60	2.62
	CH_3O	3.84	3.86	3.87	3.85

[a] Major conformational isomer.

oriented toward Tyr$^{6\alpha}$-H rather than Ala$^{1\alpha}$-H. The remaining four α protons exhibit much smaller downfield shifts of 0.09–0.18 ppm upon addition of 1.0 or 2.0 equiv LiCl. The additional perturbations may be found in the chemical shift of the strongly shielded Tyr$^{6\delta b}$-H (δ 4.55 shifted to 5.21). This loss of shielding and the maintenance of the Tyr$^{6\delta b}$-H/Tyr$^{6\alpha}$-H and Tyr$^{5\epsilon a}$-H NOE but loss of the Tyr$^{6\delta b}$-H/Tyr$^{5\epsilon b}$-H NOE suggests a small conformational change in the relative orientations of the aromatic rings of the biaryl ether with a shift of Tyr^6 from its near perfect orthogonal alignment to one more twisted with Tyr$^{6\delta b}$-H positioned closer to Tyr$^{5\epsilon a}$-H than Tyr$^{5\epsilon b}$-H. This change in the relative orientations of the aromatic rings of Tyr^6 and Tyr^5 account for the deshielding chemical shifts in Tyr$^{5\epsilon a}$ and Tyr$^{5\delta a}$ as well as the corresponding shielding chemical shifts in Tyr$^{5\epsilon b}$ and Tyr$^{5\delta b}$. Upon addition of 12 equiv of LiCl, the Ala^1-NH and Ala^2-NH continue to shift downfield, Ala^1 exhibits small further changes, Ala^2 and Tyr^6 fail to continue to change and remain relatively unchanged, and only a small perturbation in the chemical shift of Ala^4-NH and surrounding Tyr$^{3\alpha}$-H may be detected. This suggests that the tight hydrogen bond of Ala^4-NH remains relatively unperturbed. Tyr^5 is least affected throughout the addition of LiCl.

Throughout the addition of LiCl, little or no change in the coupling constants were observed including the critical region surrounding the C^{30}–N^{29} cis amide. Importantly, the coupling constants for Tyr$^{6\alpha}$-H and Tyr$^{5\alpha}$-H were not changed indicating that the backbone conformation within the cycloisodityrosine subunit was not altered.

^{1}H NMR of 9 in THF-d_8 and Complexed with LiCl in THF-d_8. Previous studies with **9** revealed that it adopts a single, rigid conformation in any NMR solvent ($CDCl_3$, CD_3OD, DMSO-d_6, THF-d_8) which possesses a trans *N*-methyl amide central to the cycloisodityrosine structure. The addition of 1–12 equiv of LiCl had no effect on this conformation of **9**, and no trace of the corresponding cis amide conformation was detected (eq 1). Thus, the cycloisodityrosine subunit of RA-VII only adopts the disfavored conformation containing a central cis *N*-methyl amide upon incorporation into the bicyclic natural product and it is the tetrapeptide housed in the 18-membered ring that induces and maintains this inherently less stable conformation.

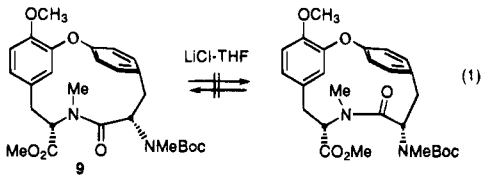

	trans : *cis*
$CDCl_3$:	100:0
CD_3OD:	100:0
DMSO-d_6:	100:0
DMF-d_7:	100:0
THF-d_8:	100:0
THF-d_8/LiCl:	100:0

Conformational Analysis. In prior studies, a very extensive and complete conformational search of **1** and **2** was conducted.[17] Global and close low lying minima (≤5.0 kcal/mol) were located by Monte Carlo sampling of starting conformations generated by random variations (0–180°) in two to six of the 18 available torsional angles in the 18-membered ring including the amide bonds.[27–29] Sixteen different minimized starting conformations were employed and constituted each accessible permutation in the stereochemistry (cis and trans) and orientation of the three *N*-methyl amides. Comparable, but less complete, results were obtained by conducting the conformational analysis with random variations in the torsional angles (0–180°) of two to four of the available six amide bonds of **1** starting with the X-ray crystal structure conformation. Using the OPLSA force field (v.3.5), the three lowest energy conformations correspond to the ctt, cct (ΔE = 1.3 kcal/mol), and ccc[30] (ΔE = 2.4 kcal/mol) conformations detected by ^{1}H NMR and parallel the relative stabilities of the three conformational isomers detected in conventional NMR solvents. Using these three conformations, a calculated Boltzmann distribution of 85:13:2 at 25 °C matches solvent dependent ratio of conformations experimentally observed remarkably well (64–88:32–12:0–4). This search provided a total of 25 conformations with 12 of the conformations containing the cis C^{30}–N^{29} amide.

Each of these 12 conformations was used as starting conformations for subsequent conformational searches[27–29] imposing the distance and torsional constraints observed in the 2D ^{1}H–^{1}H NOESY NMR. The amide geometries were fixed at cis (0° ± 10° dihedral angle) or trans (180° ± 10) to match the experimentally observed stereochemistry. In total, 35 NOE crosspeaks were obtained constituting 25 intraresidual, 8 inter-

(27) Global and close low-lying minima (≤ 5 or 12 kcal/mol, **1** and **9**, respectively) were located in conformational searches with use directed Monte Carlo sampling and subsequent minimization of conformations generated by random variations (0–180°) in the available torsional angles[28] excluding those originating in the phenyl rings (MacroModel,[29] version 3.5a, OPLSA force field, MCMM = 5000, MCSS = 2, 5, or 12 kcal/mol window). The global minima were located 30–60 times in each search.

(28) Chang, G.; Guida, W. C.; Still, W. C. *J. Am. Chem. Soc.* **1989**, *111*, 4379.

(29) Still, W. C.; Mohamadi, F.; Richards, N. G. J.; Guida, W. C.; Lipton, M.; Liskamp, R.; Chang, G.; Hendrickson, T.; DeGunst, F.; Hasel, W. *MACROMODEL* V2.7, Columbia University, New York, 1990.

(30) The notations ctt, cct, and ccc refer to the stereochemistry (c = cis, t = trans) of the C^{30}–N^{29}, C^8–N^9, and C^{14}–N^{15} *N*-methyl amides within a conformational isomer.

Table 5. $^1H-^1H$ NOE Observed with RA-VII Complexed with LiCl (1.0 equiv) in THF-d_8

crosspeak	chemical shift (δ)	intensity[a]
Ala^1-NH/Tyr$^{6\alpha}$	8.73/5.38	m
Ala^2-NH/Ala$^{1\alpha}$	8.68/4.69	m
Ala^2-NH/Ala$^{2\beta}$	8.68/1.30	m
Ala^2-NH/Ala$^{1\beta}$	8.68/1.28	m
Tyr$^{5\delta a}$/Tyr$^{5\epsilon a}$	7.56/7.35	m
Tyr$^{5\delta a}$/Tyr$^{5\alpha}$	7.56/5.60	m
Tyr$^{5\delta a}$/Tyr$^{5\beta a}$	7.56/2.56	m
Tyr$^{5\epsilon a}$/Tyr$^{6\delta b}$	7.35/5.21	w
Tyr$^{5\delta b}$/Tyr$^{5\epsilon b}$	7.10/6.60	m
Tyr$^{5\delta b}$/Tyr$^{5\beta b}$	7.10/3.49	m
Tyr$^{3\delta}$/Tyr$^{3\epsilon}$	7.06/6.81	m
Tyr$^{3\delta}$/Tyr$^{3\beta}$	7.06/3.28	s
Tyr$^{3\epsilon}$/Tyr^3-OCH$_3$	6.81/3.73	s
Tyr$^{6\epsilon a}$/Tyr$^{6\delta a}$	6.78/6.52	s
Tyr$^{6\epsilon a}$/Tyr^6-OCH$_3$	6.78/3.86	s
Ala^4-NH/Tyr^3-NCH$_3$	6.56/2.84	w
Tyr$^{5\alpha}$/Tyr$^{6\alpha}$	5.60/5.38	s
Tyr$^{5\alpha}$/Tyr$^{5\beta b}$	5.60/3.49	w
Tyr$^{5\alpha}$/Tyr$^{5\beta a}$	5.60/2.56	m
Tyr$^{6\alpha}$/Tyr$^{6\delta b}$	5.38/5.21	s
Tyr$^{6\alpha}$/Tyr$^{6\beta a}$	5.38/3.09	m
Tyr$^{6\alpha}$/Tyr$^{6\beta b}$	5.38/2.84	w
Ala$^{4\alpha}$/Tyr^5-NCH$_3$	4.85/3.04	s
Ala$^{4\alpha}$/Ala$^{4\beta}$	4.85/1.02	s
Ala$^{1\alpha}$/Ala$^{1\beta}$	4.69/1.28	s
Ala$^{1\alpha}$/Ala$^{4\beta}$	4.69/1.02	m
Ala$^{2\alpha}$/Tyr^3-NCH$_3$	4.62/2.84	s
Ala$^{2\alpha}$/Ala$^{2\beta}$	4.62/1.30	s
Tyr$^{3\alpha}$/Tyr$^{3\beta a}$	3.68/3.28	m
Tyr$^{3\alpha}$/Tyr$^{3\beta b}$	3.68/3.28	m
Tyr$^{3\alpha}$/Tyr^3-NCH$_3$	3.68/2.84	s
Tyr$^{5\beta b}$/Tyr^5-NCH$_3$	3.49/3.04	s
Tyr$^{5\beta b}$/Tyr$^{5\beta a}$	3.49/2.56	s
Tyr$^{6\beta a}$/Tyr$^{6\beta b}$	3.09/2.84	s
Tyr^3-NCH$_3$/Ala$^{2\beta}$	2.84/1.30	w

[a] s = strong, m = medium, w = weak.

Table 6. Hydrogen Bond Distances

donor	acceptor	THF-d_8/CDCl$_3$	THF-d_8/LiCl	**1** (X-ray)	**3** (X-ray)
Ala^1-NH	Ala^4-CO	2.32 Å	3.53 Å	3.24 Å	3.26 Å
Ala^4-NH	Ala^1-CO	2.38 Å	2.74 Å	2.95 Å	3.00 Å

residual, and 2 long-range peaks (Table 5). Some of the intraresidual and interresidual NOE were within the rigid cycloisodityrosine subunit (Tyr^5-Tyr^6) and constitute specific through space interactions that fix the distance, location, and assignments of the interacting nuclei. The NOE intensities were assigned relative intensities of strong, medium, or weak based on their respective volumes, and distance constraints were assigned based on fixed, calibration distances taken from the X-ray crystal structure of **1** and **3**. The upper and lower distance bounds were set at approximately ±20% of the calculated distances. This variation allows for some error in the measurement and approximation of the intensity of crosspeaks and the conversion to distances. The calculations were started with 35 assigned intensities, including calibration peaks, from the NOESY spectra. Although the results described herein were obtained with a force constant of 100 KJ/Å^2 for the restraining potential for the NOE-derived distances and with a force constant of 1000 KJ/mol for the fixed amide torsional angles, the conformational searches were also conducted independently with only one type of constraint imposed with variations in the imposed force constants without alteration in the final results. In each case, the low energy conformation located was the same, compared closely to the X-ray crystal structure conformation, and provided calculated coupling constants that match those experimentally observed. Most diagnostic of these latter comparisons was the Tyr$^{6\alpha}$-H and Tyr$^{5\alpha}$-H coupling constants within the rigid cycloisodityrosine subunit. Using the force constants listed above, seven conformations were located from each of the 12 starting conformations. Five of these conformations were 20 KJ/mol (4.8 kcal/mol) higher in energy than the low energy conformation and may be considered inaccessible or unpopulated conformations. The remaining conformation differed from the low energy conformation only by a slight skewing of the Tyr^3 aromatic ring but possessed an identical backbone conformation. The low energy conformation obtained with the distance and dihedral constraints was nearly identical to the X-ray crystal structure when comparing the 28 bicyclic backbone atoms (rms = 0.24 Å). The calculated coupling constants for Tyr$^{5\alpha}$-H (dd, J = 2.7, 11.4 Hz) and Tyr$^{6\alpha}$-H (dd, J = 1.4, 11.2 Hz) match those measured for RA-VII complexed with 1.0 equiv LiCl exceptionally well, J = 2.7, 11.3 and J = 1.4, 11.0 Hz, respectively.

The difference in the THF-d_8 solution conformation and that observed in the presence of LiCl or in the X-ray may be attributed to a weak Ala^1-NH-O=C-Ala^4 hydrogen bond. In the LiCl complexed conformation and in the X-ray, the planes defined by the Tyr^6-Ala^1 amide and the Ala^4-Tyr^5 amide are nearly perfectly parallel to each other, while the weak transannular hydrogen bond observed in common NMR solvents cause the two planes to rotate toward one another. The internuclei distance for these two hydrogen bonds are indicative of this correlation between the X-ray and LiCl complexed conformations and their distinctions from the conformation in THF-d_8 (Table 6). Models of the X-ray, THF-d_8/LiCl, and THF-d_8 conformations are illustrated in Figure 3.

Conclusions. The conformations and conformational equilibria of RA-VII and related natural products in THF-d_8 are similar to that observed in $CDCl_3$ or 15% $CD_3OD-CDCl_3$. The addition of 1 equiv of LiCl results in the adoption of a single dominant conformation (94%) that corresponds to the major conformation detected in conventional organic NMR solvents ($CDCl_3$, CD_3OD, DMSO-d_6, THF-d_8). The addition of further LiCl (1−12 equiv) has no effect on the structure or equilibria of the agent. The LiCl complexed solution conformation of RA-VII closely resembles the X-ray structure conformation. Seminal elements of this conformation include a characteristic and diagnostic cis C^{30}−N^{29} *N*-methyl amide central to a type VI β-turn and the rigid cycloisodityrosine subunit, a trans C^8−N^9 *N*-methyl amide central to a typical type II β-turn capped by a tight transannular Ala^1-C=O-HN-Ala^4 hydrogen bond, a trans C^{14}−N^{15} *N*-methyl amide, and a fully solvent accessible Ala^2-NH. Unlike the conformation observed in THF-d_8, but similar to the X-ray structure conformation, the LiCl complexed conformation of **1** lacks the weak transannular Ala^1-NH-O=C-Ala^4 hydrogen bond which results in a small perturbation in the relative orientations of the two aromatic rings of the cycloisodityrosine biaryl ether ring system. This may be attributed to preferential complexation or a preferential effect of the LiCl complexation to the Ala^1-Tyr^6 amide. Interestingly, and perhaps not fortuitous, this is the same location occupied by an ordered water in the X-ray crystal structure of **1**.[4]

In contrast, the 14-membered cycloisodityrosine **9** adopts a rigid conformation possessing a trans *N*-methyl amide central to its structure which is unaffected by the complexation with LiCl. Thus, its adoption of an inherently disfavored cis amide central to its structure within the bicyclic hexapeptide of the natural products is not solvent induced or solvent dependent.

(31) Marion, D.; Wüthrich, K. *Biochem. Biophys. Res. Commun.* **1983**, *113*, 967.

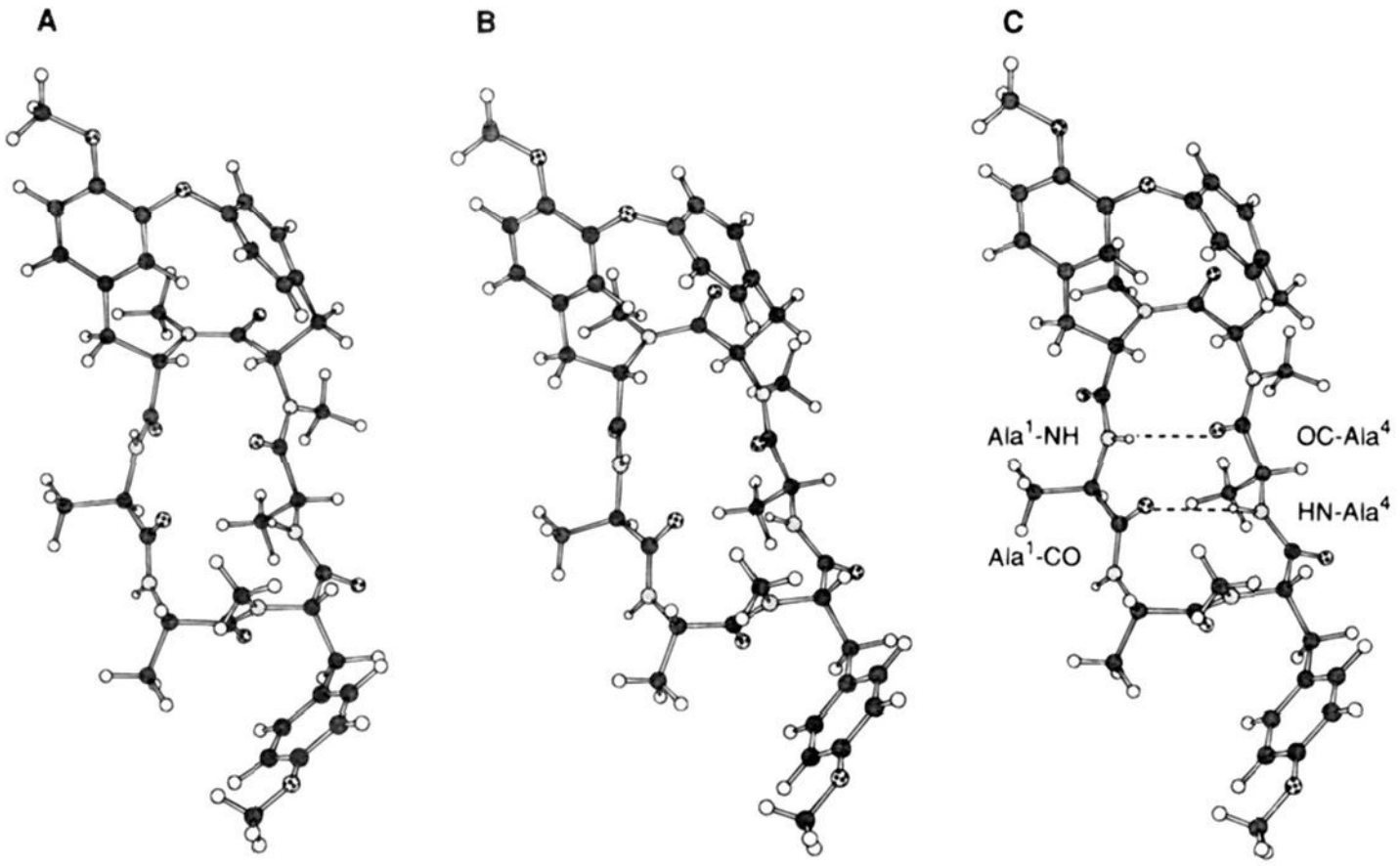

Figure 3. (A) X-ray crystal structure of RA-VII; (B) low energy conformation (THF-d_8/LiCl) from constrained Monte Carlo conformational search; (C) typical (THF-d_8) solution low energy conformation.

Experimental Section

NMR Measurements. All NMR spectra were recorded on a Bruker AMX 400 spectrometer. The sample of RA-VII (**1**) in THF-d_8 (99.95% ^{2}H atoms; CIL) was prepared by dissolving RA-VII (2.1 mg, 0.0027 mmol) in 0.5 mL of THF-d_8 in a 5-mm NMR tube. The samples of LiCl·RA-VII in THF-d_8 were prepared by treating the solution of RA-VII (**1**, 2.1 mg, 0.0027 mmol) in THF-d_8 (0.5 mL) with an appropriate volume of 0.5 M LiCl in THF-d_8 (5.4 μL, 1.0 equiv; 10.8 μL, 2.0 equiv; 64.8 μL, 12.0 equiv) in 5-mm NMR tubes. All samples were degassed by six freeze−pump−thaw cycles. All experiments were measured at 296 K. All chemical shifts are referenced to the downfield THF-d_8 signal at 3.58 ppm in the ^{1}H NMR spectra. For both uncomplexed and complexed RA-VII (**1**) in THF-d_8, 1D ^{1}H, 1D ^{1}H−^{1}H decoupling, 2D ^{1}H−^{1}H NOESY, and 2D ^{1}H−^{1}H ROESY NMR spectra were recorded. All 2D spectra were recorded with quadrature detection in both dimensions, TPPI[31] was used in F_1. The 2D spectra were processed and analyzed with the Felix program (version 2.0, Hare Research Inc.) on a Silicon Graphics Personal IRIS Workstation. The parameters of the individual NMR experiments are given in the following experimentals.

(1) 1D ^{1}H spectrum: pulse length: P1 = 5.0 μs; relaxation delay: d1 = 1.0 s; 128 acquisitions.

(2) 1D ^{1}H−^{1}H decoupling spectrum (homo-decoupler mode): pulse length: P1 = 10.0 μs; relaxation delays: D1 = 1 s, D11 = 1 ms; the power set for the decoupled nucleus (DEC): dL0 = 50 dB; 64 acquisitions.

(3) 2D ^{1}H−^{1}H NOESY spectrum: sequence D_1−90°−t_1−90°−τ_{mix}−90°−t_2; pulse length (90°): P1 = 18 μs; delays: d0 = 3 μs, d1 = 2 s, d8 = 450 ms; sweep width in F1 and F2: SWH = 4424.779 Hz; 32 acquisitions; 512 increments.

(4) 2D ^{1}H−^{1}H ROESY spectrum: Sequence D_1−90°−t_1−90°−τ_{mix}−90°−t_2. pulse lengths: P1 (90° transmitter high power pulse) = 18 μs; P15 (CW pulse for ROESY spinlock) = 400 ms; delays: d0 (incremented delay) = 3 μs, d1 (relaxation delay) = 2 s, d12 (delay for power switching) = 20 μs, d13 (short delay) = 3 μs; powers: hl1 (ecoupler high power) = 3 dB, hl4 (ecoupler low power) = 17 dB; sweep width in F1 and F2: SWH = 4424.779 Hz; 32 acquisitions; 512 increments.

Acknowledgment. We gratefully acknowledge the financial support of the National Institutes of Health (CA 41101) and the assistance of Dr. D.-H. Huang.

Supporting Information Available: A figure illustrating the ^{1}H NMR of **1** in THF-d_8, THF-d_8 + 1.0 equiv LiCl, and THF-d_8 + 2.0 equiv LiCl (1 page). This material is contained in many libraries on microfiche, immediately follows this article in the microfilm version of the journal, can be ordered from the ACS, and can be downloaded from the Internet; see any current masthead page for ordering information and Internet access instructions.

JA951059M